Hydrologic control of carbon cycling and aged carbon discharge in the Congo River basin

Enno Schefuß[1,3], Timothy I. Eglinton[2,3], Charlotte L. Spencer-Jones[4,*], Jürgen Rullkötter[5], Ricardo De Pol-Holz[6], Helen M. Talbot[4], Pieter M. Grootes[7], Ralph R. Schneider[7,8]

[1]*MARUM – Center for Marine Environmental Sciences, University of Bremen, Germany*

[2]*Department of Geological Sciences, ETH Zürich, Switzerland*

[3]*Department of Marine Chemistry and Geochemistry, Woods Hole Oceanographic Institution, USA*

[4]*School of Civil Engineering and Geosciences, Newcastle University, United Kingdom*

[5]*Institute for Chemistry and Biology of the Marine Environment (ICBM), Carl von Ossietzky University of Oldenburg, Germany*

[6]*GAIA-Antártica, Center for Climate and Resilience Research (CR)[2], Universidad de Magallanes, Punta Arenas, Chile*

[7]*Leibniz-Laboratory for Radiometric Dating and Stable Isotope Research Kiel, Germany, now at: Institute for Ecosystem Research, Christian-Albrechts-University Kiel, Germany*

[8]*Institute for Geosciences, Christian-Albrechts-University Kiel, Germany*

***Now at: Department of Geography, University of Durham, United Kingdom*

The age of organic material discharged by rivers provides information about its sources and carbon cycling processes within watersheds. While elevated ages in fluvially-transported organic matter are usually explained by erosion of soils and

sediments deposits[1,2], it is commonly assumed that mainly young organic material is discharged from flat tropical watersheds due to their extensive plant cover and rapid carbon turnover[3-7]. Here we present compound-specific radiocarbon data of terrigenous organic fractions from a sedimentary archive offshore the Congo River in conjunction with molecular markers for methane-producing land cover reflecting wetland extent. We find that the Congo River has been discharging aged organic matter for several thousand years with apparently increasing ages from the Mid- to the Late Holocene. This suggests that aged organic matter in modern samples is concealed by radiocarbon from atmospheric nuclear weapons testing. By comparison to indicators for past rainfall changes we detect a systematic control of organic matter sequestration and release by continental hydrology mediating temporary carbon storage in wetlands. As aridification also leads to exposure and rapid remineralization of large amounts of previously stored labile organic matter we infer that this process may cause a profound direct climate feedback currently underestimated in carbon cycle assessments.

Tropical humid ecosystems are hot spots of terrestrial carbon storage[8] and large river systems in tropical areas form an important conduit in the global carbon cycle by transporting vast amounts of biosynthetic OM to the ocean[9,10]. Apparent radiocarbon ages of riverine organic carbon are interpreted as the mean time elapsed since biosynthesis, integrating all intermediate storage, transport and mixing processes, and thus considered to reflect the speed of carbon cycling in watersheds. Radiocarbon studies of fluvially-transported OM reveal relatively young ages in tropical areas[3-7], suggesting rapid carbon turnover, and greater ages in temperate regions with larger influence of geomorphology and soil erosion[1,2]. Among the controlling processes, relative changes in export of contemporary biomass versus erosion of OM from soils or sedimentary rocks (e.g., refs 1,7) as well as storage in intermediate

45 reservoirs, such as floodplains and wetlands (e.g., refs 11-13), are discussed. The exact factors
46 controlling the continental residence times of terrestrial OM in tropical watersheds and their
47 response to climatic changes are, however, not yet fully understood.

48 To provide insight into the response of OM cycling in large tropical watersheds to
49 climatic changes we investigated a sedimentary archive simultaneously recording continental
50 palaeo-climatic changes and variations in terrestrial carbon cycling in the Congo basin.
51 Sediment core GeoB6518-1 (05° 35.30' S, 11° 13.30' E, 962 m water depth, Fig. 1) was
52 recovered from the Congo deep-sea fan close to the river mouth. The Congo is the second
53 largest river on Earth in terms of drainage basin size (about 3.7 x 10^6 km^2), water discharge[14]
54 and terrestrial organic matter export[15]. Located in equatorial Africa, it is characterized by low
55 intra- and inter-annual discharge variability[16]. Steep rapids close to its estuary separate the
56 central Congo basin from sea-level influence. A submarine canyon incises the continental
57 shelf, extending from the Congo estuary and leading to rapid transport of discharged material
58 to the deep-sea fan. The ages of terrestrial organic material are therefore considered to reflect
59 retention processes within the river basin. We measured the ^{14}C content of various OM
60 fractions (total organic matter, microscopic wood fragments, leaf-wax *n*-alkanes, and
61 individual leaf-wax *n*-alcohols) from several depth intervals of core GeoB6518-1 (Table S2).
62 Using the depositional ages based on radiocarbon dating of planktonic foraminifera (Table
63 S1), radiocarbon contents of OM fractions were decay-corrected to derive initial radiocarbon
64 contents. The deviation from the past atmospheric ^{14}C content ($\Delta\Delta^{14}C_{initial}$, see Methods) at the
65 time of deposition can be converted to apparent initial radiocarbon ages. The initial ages of
66 the OM fractions range from isochronous up to 3,000 ^{14}C years (Fig. 2a). Notably, initial ages
67 of wood fragments are contemporaneous to or only slightly older than depositional ages in the
68 Early to Mid-Holocene. In contrast, the plant-wax fractions are older and show higher but

69 coherent age variability (Fig. 3). This is in accordance with both a rapid transfer of plant
70 debris through the river system under high discharge conditions and the refractory nature and
71 persistence of plant waxes in soils[17]. The aged terrestrial organic contributions strongly
72 influence the age of total organic carbon (TOC) deposited off the Congo River despite its
73 mixed terrestrial and aquatic origin (Fig. 2a). From about 5,000 years before present (BP) all
74 organic components show a similar trend to greater apparent initial ages towards the present.
75 The Congo River has, thus, exported aged OM for the last several thousand years. This
76 finding is in contrast to ^{14}C results from modern fluvial OM in the Congo River and other
77 tropical river systems, where terrestrial components were found to be mainly contemporary in
78 age[4-7]. We infer that this discrepancy is caused by the influence of radiocarbon from
79 atmospheric nuclear weapons testing in modern samples, masking their original age. This
80 influence is also detected for the uppermost sample from GeoB6518-1 which exhibits
81 reversals in the $\Delta^{14}C_{initial}$ of all OM fractions (Fig. S3). The influence of bomb-derived
82 radiocarbon on modern samples in carbon cycle studies therefore needs to be considered more
83 carefully.

84 To explain the Holocene age variations we investigated indicators for OM contributions
85 from soils, sedimentary rocks and wetlands, and also considered variable carbon turnover due
86 to changes in river transport, continental temperatures and hydrologic conditions. Previously
87 we showed that the OM of core GeoB6518-1 is predominantly terrigenous with the majority
88 derived from soils[18]. The proportion of soil- versus plant-derived OM estimated by the
89 abundance of membrane lipids from soil-hosted bacteria, however, was relatively invariant
90 through time[18] (Table S2). While this suggests that relative contribution changes of soil-
91 derived OM due to variable vegetation cover and soil erosion cannot explain the age
92 variations, it does not rule out erosion of deep soil layers and intermediate deposition and re-

93 suspension during riverine transport as potential processes leading to elevated ages.
94 Nevertheless, we regard these effects as minor considering the relatively flat geomorphology
95 of the Congo basin[14], the Congo's high discharge even under today's relatively dry conditions
96 and the observation that similar age variations were also detected for wood fragments (Fig.
97 2a, 3, 4). Similarly, we rule out an influence of fossil OM contributions from sedimentary
98 rocks as the molecular composition of the plant-wax fractions does not show any indication of
99 thermally mature hydrocarbons (Fig. S1). Also, we infer that hydraulic sorting of fine and
100 coarse particles carrying different radiocarbon contents[5] cannot explain the observed ages as
101 variations were also detected for the coarse (> 150 μm) wood fragments. As no large
102 continental temperature variations in central Africa occurred during the Holocene[19] (Fig. 2b),
103 we also exclude temperature-driven changes in soil carbon turnover[8,20] as an explanation for
104 the observed age variations. Instead, we observe a strong relation to changes in continental
105 hydrology. In particular, the trend towards greater ages from the Mid- to Late Holocene is
106 paralleled by the aridification trend in central Africa[21] (Fig. 2c). Towards the relatively dry
107 present-day conditions all terrestrial OM fractions converge to their greatest initial ages.
108 Comparing the radiocarbon contents of the molecular OM fractions to the hydrogen stable
109 isotope compositions (δD) of the *n*-C_{24} alcohol as a measure of rainfall intensity[21], reveals that
110 initial ages significantly increased when δD values exceeded -145 ‰ VSMOW, indicating
111 more arid conditions (Fig. 4). We thus conclude that the observed age trend was caused by
112 release of previously stored OM from intermediate reservoirs controlled by changes in
113 continental hydrology. Despite the high coverage of the Congo basin by tropical rainforest,
114 even the deposited wood fragments follow this trend, suggesting a massive release of aged
115 terrestrial OM. Disentangling the sedimentary TOC into pre-aged and fresh portions, i.e.,
116 directly from plants and aquatic organisms, reveals that about 30 to 70 % of TOC is pre-aged
117 during the Early to Mid-Holocene while this portion increases to 70 to 90 % in the Late

Holocene (Fig. 2d). Accumulation rates of pre-aged OC at GeoB6518-1 (Fig. 2e) are higher during the latest Holocene than during the wetter Early to Mid-Holocene suggesting strongly increased export fluxes of pre-aged OM by the Congo River under more arid conditions.

In order to identify the source of this large-scale old OM release, we analysed bacterial signature lipids, i.e., bacteriohopanepolyols (BHPs)[22,23], in sediments of GeoB6518-1. In particular, we focused on 35-aminobacteriohopane-30,31,32,33,34-pentol (aminopentol), a marker for aerobic methanotrophic bacteria predominant in wetlands[22]. Strong similarities of the BHP signature in the Congo deep-sea fan and in wetland deposits[22,23] (Fig. S2), coupled with limited ^{13}C depletion of the BHPs, are consistent with aerobic oxidation of methane in a terrestrial setting[23] (see supplement). The aminopentol abundance profile in GeoB6518-1 (Fig. 2f) reveals a striking resemblance to the continental hydrologic changes[21] (Fig. 2c). In the humid Early Holocene, maximum abundance of aminopentol indicates largest wetland extent in the Congo basin while its decreasing abundance suggests shrinking methane-producing land cover during the Mid- to Late Holocene concomitant with increasing initial ages of terrestrial OM (Fig. 2a). The observed threshold-like age trend with decreasing rainfall intensity (Fig. 4) may point to an environmental tipping point with respect to wetland extent depending on the regional geomorphology of the basin. The most likely candidate for such a wetland system is the Cuvette Congolaise in the vast central depression of the Congo basin at the confluence of several tributaries. It hosts one of the World's largest swamp forests containing seasonally and permanently flooded wetlands with an estimated area of 360,000 km^2 (ref 24) (Fig. 1). These wetlands receive plant OM from local and upstream sources and accumulate substantial amounts of OM[25,26]. Having remained largely unnoticed until recently[27,28], the modern central Congo basin is estimated to store at least 9 Pg C[28] as a consequence of water-saturated wetland soils inhibiting aerobic OM decomposition and

instead resulting in (slower) anaerobic degradation emitting methane and other greenhouse gases[29].

These various lines of evidence suggest that areas of OM storage under anoxic conditions and associated methane production in the central Congo basin were more extended during the more humid Early Holocene, serving as an important locus of temporary storage of plant biomass. More rainfall in the basin led to higher transport of plant organic material into the Cuvette Congolaise where it accumulated in the vast permanently flooded swamp forest areas. In water-logged wetland soils remineralisation is diminished leading to enhanced preservation and storage of OM. The elevated ages of refractory plant-wax lipids even under wet, high discharge conditions point to additional processes, such as intermediate storage during fluvial transport and /or deep soil erosion, affecting their ages. Upon aridification, permanently flooded wetland areas with methane-producing land cover contracted and previously anoxic deposits eroded triggering release of aged terrestrial OM. Additionally, lower water levels caused erosion of deeper soil layers and previously deposited river beds. Exposure of OM previously stored under anoxic conditions not only leads to release of refractory organic components which are discharged but also of labile OM that is rapidly oxidized. Thus, in addition to decreasing carbon sequestration due to wetland shrinkage, the release and remineralisation of labile OM introduces a direct climatic feedback under more arid conditions, the magnitude of which remains uncertain. Given that most tropical watersheds, such as the Amazon[27], contain extended wetland areas these findings have profound global implications for the response of tropical terrestrial carbon inventories and carbon cycle feedbacks upon hydrological changes. Impacted by natural climatic changes as well as anthropogenic activities such as land use, deforestation, rising CO_2 levels and associated effects on climate[30], any changes in tropical wetland extent may thus exert a direct

166 climatic feedback. Presently, such effects are underestimated in global climate assessments[30]
167 and must be considered to more accurately assess the response of terrestrial carbon cycle
168 dynamics to future climatic change.

169

References

1 Raymond, P. A. & Bauer, J. E. Riverine export of aged terrestrial organic matter to the North Atlantic Ocean. *Nature* **409**, 497-500 (2001).

2 Hilton, R. G. *et al.* Climatic and geomorphic controls on the erosion of terrestrial biomass from subtropical mountain forest. *Glob. Biogeochem. Cycles* **26**, doi:10.1029/2012gb004314 (2012).

3 Hedges, J. I. *et al.* Organic carbon-14 in the Amazon River system. *Science* **231**, 1129-1131 (1986).

4 Martin, E. E. *et al.* Age of riverine carbon suggests rapid export of terrestrial primary production in tropics. *Geophys.Res. Lett.* **40**, 5687-5691 (2013).

5 Spencer, R. G. M. *et al.* An initial investigation into the organic matter biogeochemistry of the Congo River. *Geochim. Cosmochim. Acta* **84**, 614-627 (2012).

6 Galy, V. & Eglinton, T. Protracted storage of biospheric carbon in the Ganges-Brahmaputra basin. *Nature Geosci.* **4**, 843-847 (2011).

7 Marwick, T. R. *et al.* The age of river-transported carbon: A global perspective. *Glob. Biogeochem. Cycles* **29**, GB004911 (2015).

8 Carvalhais, N. *et al.* Global covariation of carbon turnover times with climate in terrestrial ecosystems. *Nature* **514**, 213-217 (2014).

9 Huang, T. H., Fu, Y. H., Pan, P. Y. & Chen, C. T. A. Fluvial carbon fluxes in tropical rivers. *Curr. Opin. Environ. Sustain.* **4**, 162-169 (2012).

10 Schluenz, B. & Schneider, R. R. Transport of terrestrial organic carbon to the oceans by rivers: re-estimating flux- and burial rates. *Int. J. Earth Sci.* **88**, 599-606 (2000).

11 Blair, N. E., Leithold, E. L. & Aller, R. C. From bedrock to burial: the evolution of particulate organic carbon across coupled watershed-continental margin systems. *Mar. Chem.* **92**, 141-156 (2004).

12 Kusch, S., Rethemeyer, J., Schefuß, E. & Mollenhauer, G. Controls on the age of vascular plant biomarkers in Black Sea sediments. *Geochim. Cosmochim. Acta* **74**, 7031-7047 (2010).

13 Drenzek, N. J. *et al.* A new look at old carbon in active margin sediments. *Geology* **37**, 239-242 (2009).

14 Runge, J. The Congo River, Central Africa. in *Large Rivers: Geomorphology and Management* (ed A. Gupta) 293-309 (Wiley, 2007).

15 Coynel, A., Seyler, P., Etcheber, H., Meybeck, M. & Orange, D. Spatial and seasonal dynamics of total suspended sediment and organic carbon species in the Congo River. *Glob. Biogeochem. Cycles* **19**, GB4019 (2005).

16 Laraque, A., Bricquet, J. P., Pandi, A. & Olivry, J. C. A review of material transport by the Congo River and its tributaries. *Hydrol. Process.* **23**, 3216-3224 (2009).

17 Huang, Y., Li, B., Bryant, C., Bol, R. & Eglinton, G. Radiocarbon dating of aliphatic hydrocarbons: a new approach for dating passive-fraction carbon in soil horizons. *Soil Sci. Soc. Am. J.* **63**, 1181-1187 (1999).

18 Weijers, J. W. H., Schouten, S., Schefuss, E., Schneider, R. R. & Sinninghe Damsté, J. S. Disentangling marine, soil and plant organic carbon contributions to continental margin sediments: A multi-proxy approach in a 20,000 year sediment record from the Congo deep-sea fan. *Geochim. Cosmochim. Acta* **73**, 119-132 (2009).

19 Weijers, J. W. H., Schefuss, E., Schouten, S. & Sinninghe Damsté, J. S. Coupled thermal and hydrological evolution of tropical Africa over the last deglaciation. *Science* **315**, 1701-1704 (2007).

20 Davidson, E. A. & Janssens, I. A. Temperature sensitivity of soil carbon decomposition and feedbacks to climate change. *Nature* **440**, 165-173 (2006).

21 Schefuß, E., Schouten, S. & Schneider, R. R. Climatic controls of Central African hydrology during the last 20,000 years. *Nature* **437**, 1003-1006 (2005).

22 Spencer-Jones, C. L. *et al.* Bacteriohopanepolyols in tropical soils and sediments from the Congo River catchment area. *Org. Geochem.* **89-90**, 1-13 (2015).

23 Talbot, H. M. *et al.* Variability in aerobic methane oxidation over the past 1.2 Myrs recorded in microbial biomarker signatures from Congo fan sediments. *Geochim. Cosmochim. Acta* **133**, 387-401 (2014).

24 Bwangoy, J. R. B., Hansen, M. C., Roy, D. P., De Grandi, G. & Justice, C. O. Wetland mapping in the Congo Basin using optical and radar remotely sensed data and derived topographical indices. *Remote Sens. Environ.t* **114**, 73-86 (2010).

25 Mitsch, W. J. *et al.* Wetlands, carbon, and climate change. *Landsc. Ecol.* **28**, 583-597 (2013).

26 Kayranli, B., Scholz, M., Mustafa, A. & Hedmark, A. Carbon storage and fluxes within freshwater wetlands: a critical review. *Wetlands* **30**, 111-124 (2010).

27 Keddy, P. A. *et al.* Wet and wonderful: The World's largest wetlands are conservation priorities. *Bioscience* **59**, 39-51 (2009).

28 Joosten, H. & Tapio-Biström, M.-L. Peatlands - guidance for climate change mitigation through conservation, rehabilitation and sustainable use. in *Mitigation of climate change in agriculture* Vol. 5 100 pp. (Food and Agriculture Organization of the United Nations/Wetlands International, Rome, 2012).

29 Borges, A. V. *et al.* Globally significant greenhouse-gas emissions from African inland waters. *Nature Geosci.* **8**, 637-642 (2015).

30 Arneth, A. *et al.* Terrestrial biogeochemical feedbacks in the climate system. *Nature Geosci.* **3**, 525-532 (2010).

Correspondence and requests for materials

Correspondence and requests for materials should be addressed to E.S. (eschefuss@marum.de).

Acknowledgements

We thank J. M. Hayes, G. Mollenhauer, T. Goldhammer, M. Zabel, T. Wagner and M. Schulz for discussions. M. Luttmann, H. Buschhoff, D. Montluçon, F. Sidgwick, P. Green and S. Sylva are thanked for analytical support. We thank the staff at all involved radiocarbon dating facilities for their invaluable efforts. This study was supported by the Deutsche Forschungsgemeinschaft (grants SCHN 621/3-3, RU 458/29-3, GR 1845/2-3, SCHE 903/1), the US National Science Foundation (grant OCE-0137005), a Starting Grant from the European Research Council (ERC) awarded to HMT for project AMOPROX (No. 258734) and grants ICM-NC120066 and FONDAP15110009 to RDP-H. This work was supported by the DFG Research Center/Cluster of Excellence 'The Ocean in the Earth System' at MARUM – Center for Marine Environmental Sciences, University of Bremen.

Author contributions

E.S., T.I.E., J.R., P.M.G., and R.R.S. designed the study. Analytical work was performed by E.S., C.L.S.-J., H.M.T., J.R., P.M.G., and R.D.P.-H.. E.S. wrote the manuscript approved by all co-authors.

Competing financial interests

The authors declare no competing financial interests.

Figure captions

Figure 1: The Congo River basin in central Africa. Redrawn after ref 14. Light grey areas are lakes. Dark grey area is the present-day extent of swamp forest in the Cuvette Congolaise[24,27]. Black star offshore the Congo River mouth is sampling location of sediment core GeoB6518-1.

Figure 2: OM ages offshore the Congo River and central African environmental changes. a) Offsets in radiocarbon contents versus the past atmosphere and apparent initial ages at time of deposition (brown: wood pieces, green: *n*-C_{24} alcohol, grey: *n*-alkanes, blue: TOC), error bars show analytical uncertainty propagated with $\Delta^{14}C_{atm}$ uncertainty, b) estimates of past temperatures[19], c) hydrogen stable isotope composition of *n*-C_{29} alkane[21] reflecting rainfall intensity, green dots: *n*-C_{24} alcohol, error bars show analytical uncertainty, d) TOC disentangled in fresh (green) and pre-aged (brown) portions, e) accumulation rate of pre-aged OC, f) abundance of aminopentol reflecting extent of methane-producing landcover[23].

Figure 3: Correlation of age variations between different OM fractions. Initial radiocarbon offsets are strongly correlated ($r = 0.93$, $p < 0.05$) for *n*-alkanes (grey dots) and *n*-C_{24} alcohol indicating that both are affected by the same continental retention processes. Error bars show analytical uncertainty propagated with $\Delta^{14}C_{atm}$ uncertainty. Radiocarbon offsets are more negative for *n*-alkanes than for *n*-C_{24} alcohol indicating that *n*-alkanes are more refractory than *n*-C_{24} alcohol. Radiocarbon

offsets of wood fragments (brown dots) show no correlation to initial radiocarbon offsets of *n*-C_{24} alcohol except for the lowest initial radiocarbon offsets, i.e., highest apparent initial ages.

Figure 4: Relation between rainfall intensity and OM ages. Comparison of initial radiocarbon offsets of wood pieces (brown dots) and *n*-C_{24} alcohol (green dots) with hydrogen isotope compositions of *n*-C_{24} alcohol. Error bars show analytical uncertainty propagated with $\Delta^{14}C_{atm}$ uncertainty. Initial radiocarbon offsets of *n*-alkanes (Fig. 3) and TOC show the same trend but are omitted for clarity. Where the hydrogen stable isotope composition of the *n*-C_{24} alcohol exceeds -145 ‰ VSMOW, initial radiocarbon offsets of all OM fractions become more negative indicating release of previously stored, i.e., pre-aged, material.

Online Content Methods are available in the online version of the paper; references unique to this section appear only in the online paper. Source data and additional display items are in the Supplementary Information.

Methods

Age model of GeoB6518-1. The age model of GeoB6518-1 is based on AMS dating of mixed planktonic foraminifera containing *Globigerinoides ruber* (white), *Globigerinoides sacculifer* and *Orbulina universa* isolated from sediments by wet-sieving (> 150 μm) and picking. Fractions were cleaned with H_2O and 15% H_2O_2, carbonate was converted to CO_2 with 100% phosphoric acid and subsequently catalytically reduced to graphite for AMS measurement of radiocarbon (^{14}C) contents. ^{14}C contents were corrected for blank effects[31] (Table S1). Most foraminiferal ages were reported earlier[21] and re-calibrated to calendar ages in this study. An additional age point was added for depth 128-138 cm. A further sample (78-88 cm) was lost during AMS measurement. All dates were calibrated with Calib7.0 using the Marine13 radiocarbon age calibration and no regional and temporal offset in the reservoir age correction[32]. We set the mid-point of the sampling interval to the mean age of the calibrated 2-σ age interval. Because the uppermost sample (5-15 cm) contains radiocarbon from atmospheric nuclear weapons testing (post-1950 age), we set the core-top to zero age and did not regard the uppermost sample as an age tie-point. Ages of individual samples between tie-points were linearly interpolated.

Radiocarbon dating of total organic carbon and wood fragments. Total organic carbon (TOC) contents (Tables S2, S3, S4) were determined by combustion of ground and de-carbonated sediment samples at 1050°C using a Leco CS230 Carbon-Sulphur analyser. The relative precision of the measurements, based on triplicate analyses was better than 1.8% relative standard deviation. For ^{14}C analyses of TOC, ground sediments were treated with 1%

329 hydrochloric acid to remove carbonates and subsequently freeze-dried. Samples were
330 combusted with copper oxide and silver wool in quartz tubes and the CO_2 released converted
331 into graphite for AMS measurement. ^{14}C contents were corrected for blank contributions[31].
332 Several microscopic wood fragments (> 150 µm) were isolated from each sediment sample
333 under a binocular microscope. After acid-base-acid treatment to remove humic materials they
334 were combusted and the resulting CO_2 catalytically converted to graphite for ^{14}C
335 measurement by AMS. ^{14}C contents were corrected for blank contributions and small sample
336 size[33]. Two samples (253-258 cm, 453-458 cm) yielded ages of wood pieces younger than
337 depositional ages. This may be due to slight variations in the marine reservoir age. Therefore,
338 their corresponding ^{14}C data were omitted from further calculations. As these data derive from
339 deglacial and early Holocene samples, omitting them from discussion has no influence on the
340 observation of increasing wood ages towards the Late Holocene. Data are listed in
341 supplementary Table S2.

342 **Radiocarbon dating of plant-waxes.** Sediments were Soxhlet-extracted with a 93:7 mixture
343 of dichloromethane and methanol and afterwards saponified with 0.5 M KOH in methanol.
344 After re-extraction with hexane, neutral fractions were separated by liquid chromatography
345 over silica-gel (SiO_2) columns into apolar, ketone and polar fractions by elution with hexane,
346 hexane/dichloromethane and methanol, respectively. Elemental sulphur was removed from
347 apolar fractions using activated copper before branched and cyclic lipids were removed by
348 urea adduction. Unsaturated compounds were removed by liquid chromatography over
349 $AgNO_3$-impregnated SiO_2 columns. *n*-Alkane fractions were quantified against external
350 alkane standards via gas chromatography-flame ionisation detection (GC-FID) and
351 quantitatively transferred into quartz tubes, combusted and the produced CO_2 catalytically
352 converted into graphite before AMS measurement. Alcohol fractions were acetylated with
353 acetic anhydride with known isotopic composition and treated by urea adduction and $AgNO_3$-
354 SiO_2 chromatography. After GC-FID quantification, the *n*-C_{24} alcohol was isolated by
355 preparative gas chromatography using a gas chromatograph coupled to a preparative fraction
356 collector[34]. After cleaning the isolated compounds by silica-gel column chromatography,

aliquots were checked for purity by GC-FID and samples were transferred into quartz tubes, combusted and the produced CO_2 catalytically converted into graphite for AMS measurement. ^{14}C contents were corrected for modern and fossil blank contributions to small samples by error propagation. *n*-Alcohol radiocarbon contents were corrected for carbon contribution from the added acetate group by mass balance calculation. The hydrogen isotope ratio of the *n*-C_{24} alcohol was measured using a mass spectrometer connected to a gas chromatograph via a pyrolysis interface against H_2 reference gas. The H_3-factor was measured daily and was < 6 ppm mV^{-1} with variability from day to day of less than 0.2 ppm mV^{-1}. Analyses of an external alkane standard ("Arndt B", Arndt Schimmelmann, Indiana State University) revealed a mean absolute precision of 3 ‰ and an accuracy of 0 ‰. Precision of δD composition of the *n*-C_{24} alcohol is based on replicate analyses. The δD value of the *n*-C_{24} alcohol was corrected for the added acetate group by mass-balance calculation. Data are listed in supplementary Table S2.

Calculation of initial $\Delta\Delta^{14}C$ and apparent initial ages. If the depositional age is known, i.e., the calendar age derived from the planktonic foraminifera, it is possible to calculate the initial radiocarbon content from the measured fraction modern (Fm) of all OM AMS results (Table S2) using the following equation[35]:

$$\Delta^{14}C_{inital} = (Fm\ e^{(\lambda t)} - 1) \times 1000\ ‰$$

Fm is the measured fraction modern, λ is the decay constant (1/8267 $years^{-1}$) of ^{14}C, and t is time since deposition in years. For the sampling depth for which the foraminiferal ^{14}C sample was lost (78-88 cm), we assumed the depth-integrated age from the linear interpolation (2492 ± 354 calendar years) as depositional age in order to be able to calculate initial radiocarbon contents of different OM fractions.

The offset of the initial radiocarbon contents of OM fractions to that of the past atmosphere ($\Delta^{14}C_{atm}$) is calculated as:

$$\Delta\Delta^{14}C_{initial} = \Delta^{14}C_{initial} - \Delta^{14}C_{atm}$$

$\Delta^{14}C$ values for the past atmosphere are based on time-integrated values derived from the Intcal13 southern Hemisphere atmospheric data[36]. For the uppermost sample (5-15 cm), which contains nuclear bomb-derived radiocarbon, we obtained the atmospheric ^{14}C content from the atmospheric measurements[37] at the year of core retrieval (year 2000 CE). The associated error for this sample was obtained from the corresponding ages of the sample depth interval[37]. $\Delta^{14}C_{atm}$ values are given in Table S2.

In order to provide ages instead of only radiocarbon contents, the apparent initial (conventional) ^{14}C age is calculated from the initial radiocarbon content[35]:

$$^{14}C \text{ age} = -8033 \times \ln [(1 + \Delta^{14}C_{initial}/1000)/(1 + \Delta^{14}C_{atm}/1000)] \; ^{14}C \text{ years}$$

with $\Delta^{14}C_{initial}$ the initial radiocarbon content of each OM fraction and $\Delta^{14}C_{atm}$ the atmospheric radiocarbon content at the time of deposition.

Estimates of pre-aged OC fractions and accumulation rates. To provide estimates of the relative and absolute release of previously deposited, i.e., aged, organic matter, we conducted a mass-balance calculation using the amount and initial ^{14}C contents of TOC and the initial ^{14}C contents of plant-wax *n*-alkanes and of the past atmosphere (Table S2) to disentangle fresh from pre-aged portions within TOC.

$$\text{Pre-aged OC \%} = \text{TOC \%} \times (\Delta^{14}C_{TOC\_initial} - \Delta^{14}C_{atm}) / (\Delta^{14}C_{alkanes\_initial} - \Delta^{14}C_{atm})$$

with TOC = TOC content of sample, $\Delta^{14}C_{TOC\_initial}$ = decay-corrected past ^{14}C contents of TOC, $\Delta^{14}C_{atm}$ = past atmospheric ^{14}C contents, $\Delta^{14}C_{alkanes\_initial}$ = decay-corrected past ^{14}C contents of *n*-alkanes (all data in Table S2).

The *n*-alkanes as oldest dated fractions in all sediment samples were taken as representing the age of released organic material acknowledging that also these compounds contain fresh portions, i.e., directly derived from plants. As TOC also contains aquatic OM of modern origin albeit in small amounts[18] which adds to the estimated fresh portion of TOC this results in a slight over-estimation of the fresh, directly plant-derived OM. Additionally, it must be

considered that the labile OM, which is released from wetland deposits, is rapidly oxidised (see main text) and will not be preserved in sedimentary archives. The estimates of pre-aged sedimentary TOC portions therefore reflect minimum estimates of released organic matter.

To evaluate if not only the relative portion of pre-aged OC in the sedimentary archive increased but also the absolute flux of pre-aged material, we calculated the accumulation rate of pre-aged OC in the sediment given by the percentage of pre-aged OC multiplied by the bulk sediment accumulation rate (bulk accumulation rate = sedimentation rate x dry bulk density). While we acknowledge that the accumulation rates of all sedimentary components are strongly dominated by the sedimentation rate (see supplementary Fig. S3d) it is clear that the accumulation rate of pre-aged OC in the latest Holocene exceeds its values during the Early and Mid-Holocene suggesting that also the export flux of pre-aged OC by the Congo River is higher under most arid conditions.

Influence of fossil plant-wax contributions. In order to evaluate if the higher plant-wax ages were caused by variable admixture of fossil, i.e., petrogenic, contributions, we calculated the Carbon Preference Index (CPI)[38]:

$$CPI = 0.5 \times (\Sigma(C_i + C_{i+2} + .. + C_n) / \Sigma(C_{i-1} + C_{i+1} + .. + C_{n-1}) + \Sigma(C_i + C_{i+2} + .. + C_n) / \Sigma(C_{i+1} + C_{i+3} + .. + C_{n+1}))$$

where i is the number of carbon atoms. CPI was calculated for *n*-alkanes ranging from i = 27 to n = 33 and for *n*-alcohols from i = 22 to n = 28. Terrestrial higher plants produce long-chain *n*-alkanes with elevated CPI values[38] whereas thermally altered and extensively degraded organic matter contains *n*-alkanes with a CPI around 1 (ref 39). CPI indices of *n*-alkanes and *n*-alcohols do not correlate with their initial radiocarbon content (see supplementary Fig. S1). Therefore, we rule out that the observed age variations reflect contributions of petrogenic material from eroded sedimentary rocks.

Bacteriohopanepolyols. Full details of the BHP methodology were published previously[23,40]. Briefly, total lipids were extracted from freeze-dried sediments using a modified Bligh and

Dyer technique. One third of the extract was then acetylated to yield acetylated BHPs, which were analysed by reversed-phase high performance liquid chromatography-atmospheric pressure chemical ionisation-mass spectrometry (HPLC-APCI-MS^n). Semi-quantification of BHP contents was achieved employing the characteristic base peak areas of individual BHPs in mass chromatograms relative to the *m/z* 345 mass chromatogram base peak area of the acetylated 5α-pregnane-3β,20β-diol internal standard. Averaged relative response factors relative to the internal standard, determined from a suite of acetylated BHP standards, were used to adjust the BHP peak areas. Typical error in absolute quantification was ± 20%, based on selected replicate analyses and BHP standards of known concentration[23,40]. BHP data are in supplementary tables S3, S4 and supplementary figure S2.

Data availability. Data generated in this study are available from the PANGAEA database (https://doi.pangaea.de/10.1594/PANGAEA.862021).

References only in Methods

31 Nadeau, M.-J. *et al.* Sample throughput and data quality at the Leibniz-Labor AMS facility. *Radiocarbon* **40**, 239-245 (1998).

32 Reimer, P. J. *et al.* INTCAL13 and MARINE13 radiocarbon age calibration curves 0-50,000 years cal BP. *Radiocarbon* **55**, 1869-1887 (2013).

33 Santos, G. M., Southon, J. R., Griffin, S., Beaupre, S. R. & Druffel, E. R. M. Ultra small-mass AMS C-14 sample preparation and analyses at KCCAMS/UCI Facility. *Nucl. Instrum. Methods Phys. Res. B* **259**, 293-302 (2007).

34 Eglinton, T. I., Aluwihare, L. I., Bauer, J. E., Druffel, E. R. M. & McNichol, A. P. Gas chromatographic isolation of individual compounds from complex matrices for radiocarbon dating. *Anal. Chem.* **68**, 904-912 (1996).

35 Stuiver, M. & Polach, H. A. Discussion: Reporting of ^{14}C data. *Radiocarbon* **19**, 355-363 (1977).

36 Hogg, A. G. *et al.* SHCAL13 southern hemisphere calibration, 0-50,000 years cal BP. *Radiocarbon* **55**, 1889-1903 (2013).

37 Levin, I., Kromer, B. & Hammer, S. Atmospheric Delta (CO2)-C-14 trend in Western European background air from 2000 to 2012. *Tellus Ser. B* **65**, 20092 (2013).

38 Eglinton, G. & Hamilton, R. J. Leaf epicuticular waxes. *Science* **156**, 1322-1335 (1967).

39 Peters, K. E. & Moldowan, J. M. *The Biomarker Guide: Interpreting Molecular Fossils in Petroleum and Ancient Sediments*. (Prentice-Hall, 1993).

40 van Winden, J. F. *et al.* Bacteriohopanepolyol signatures as markers for methanotrophic bacteria in peat moss. *Geochim. Cosmochim. Acta* **77**, 52-61 (2012).

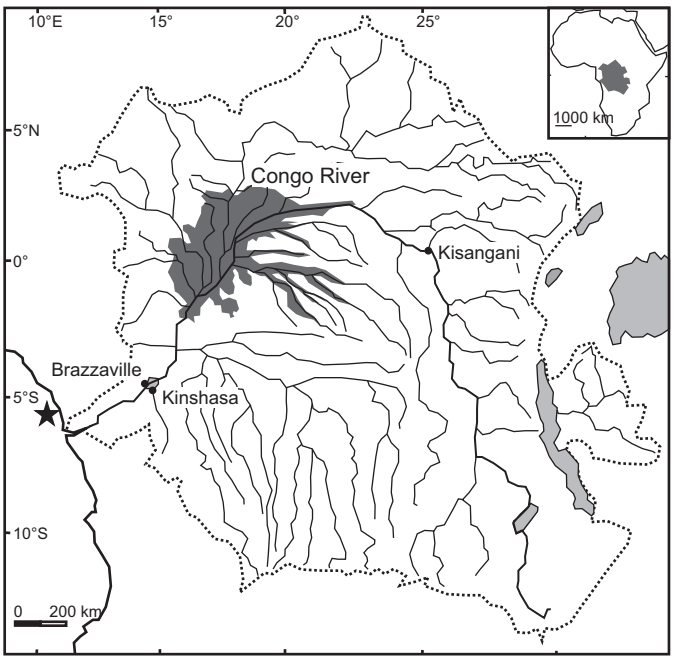
10°E
15°
20°
25°
5°N
0°
5°S
10°S
Congo River
Kisangani
Brazzaville
Kinshasa
0 200 km
1000 km

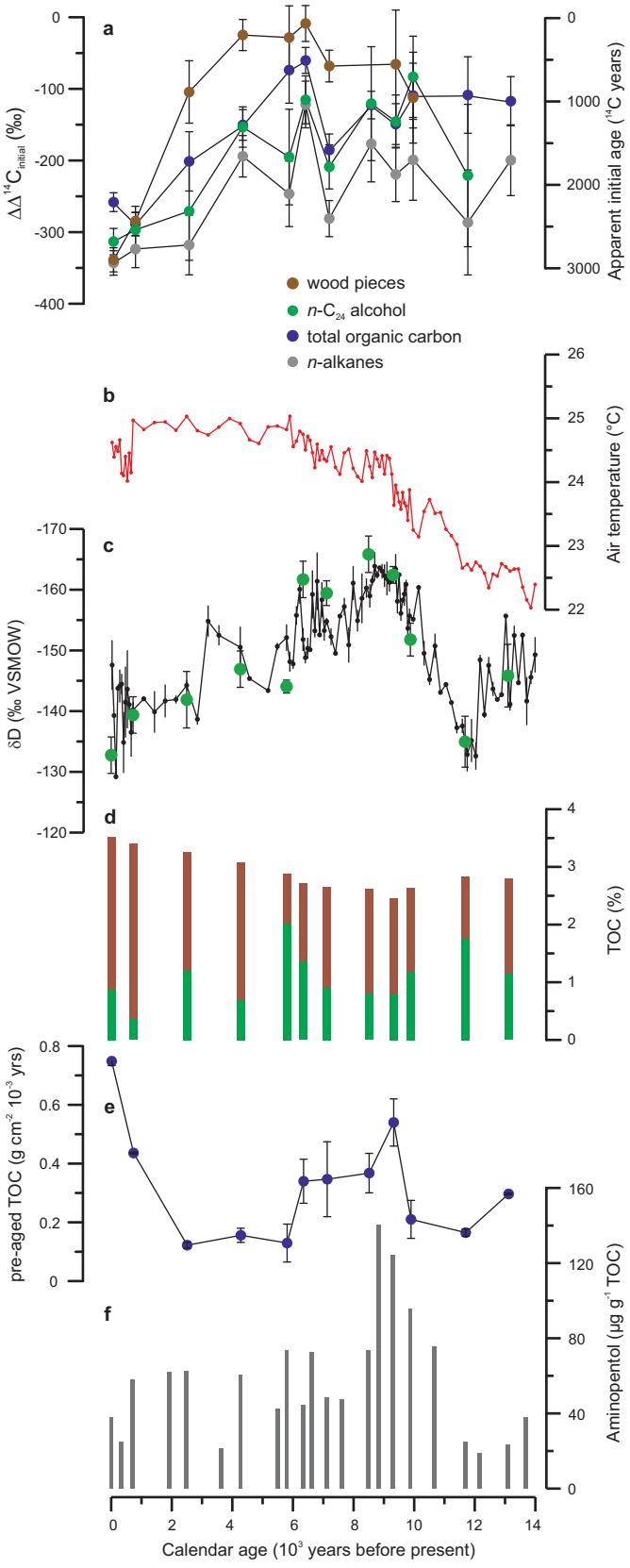
a
b
c
d
e
f
wood pieces
n-C24 alcohol
total organic carbon
n-alkanes
ΔΔ14Cinitial (‰)
Apparent initial age (14C years)
Air temperature (°C)
δD (‰ VSMOW)
TOC (%)
pre-aged TOC (g cm-2 10-3 yrs)
Aminopentol (µg g-1 TOC)
Calendar age (10³ years before present)

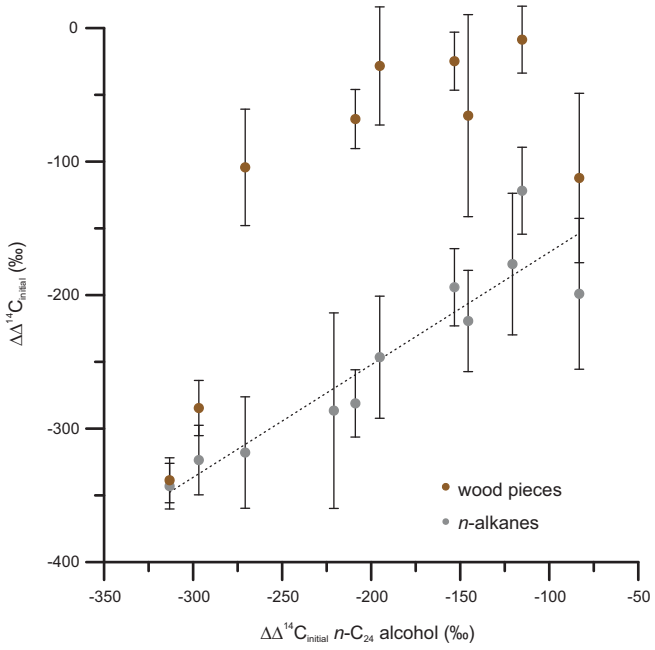
0
-100
-200
-300
-400
-350
-300
-250
-200
-150
-100
-50
ΔΔ14Cinitial (‰)
ΔΔ14Cinitial n-C24 alcohol (‰)
wood pieces
n-alkanes

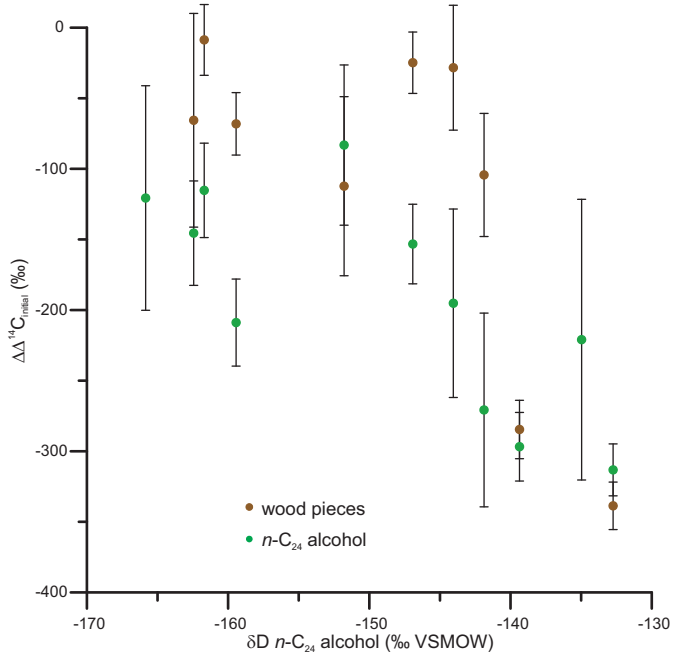
0
-100
-200
-300
-400
-170
-160
-150
-140
-130
ΔΔ 14C initial (‰)
δD n-C24 alcohol (‰ VSMOW)
wood pieces
n-C24 alcohol

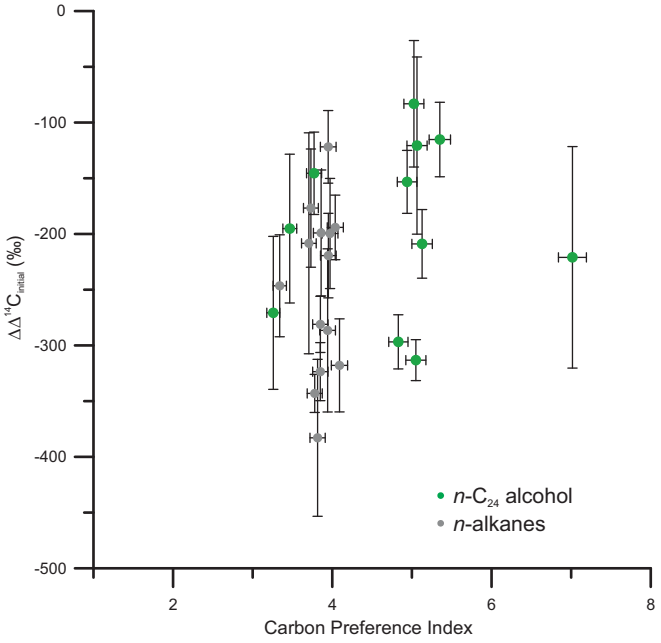

Figure S1: Absence of fossil OM influences on OM ages. Initial radiocarbon offsets of *n*-alkanes (grey dots) and *n*-C_{24} alcohol (green dots) versus their respective Carbon-Preference-Indices (CPI), error bars show analytical uncertainty propagated with $\Delta^{14}C_{atm}$ uncertainty.

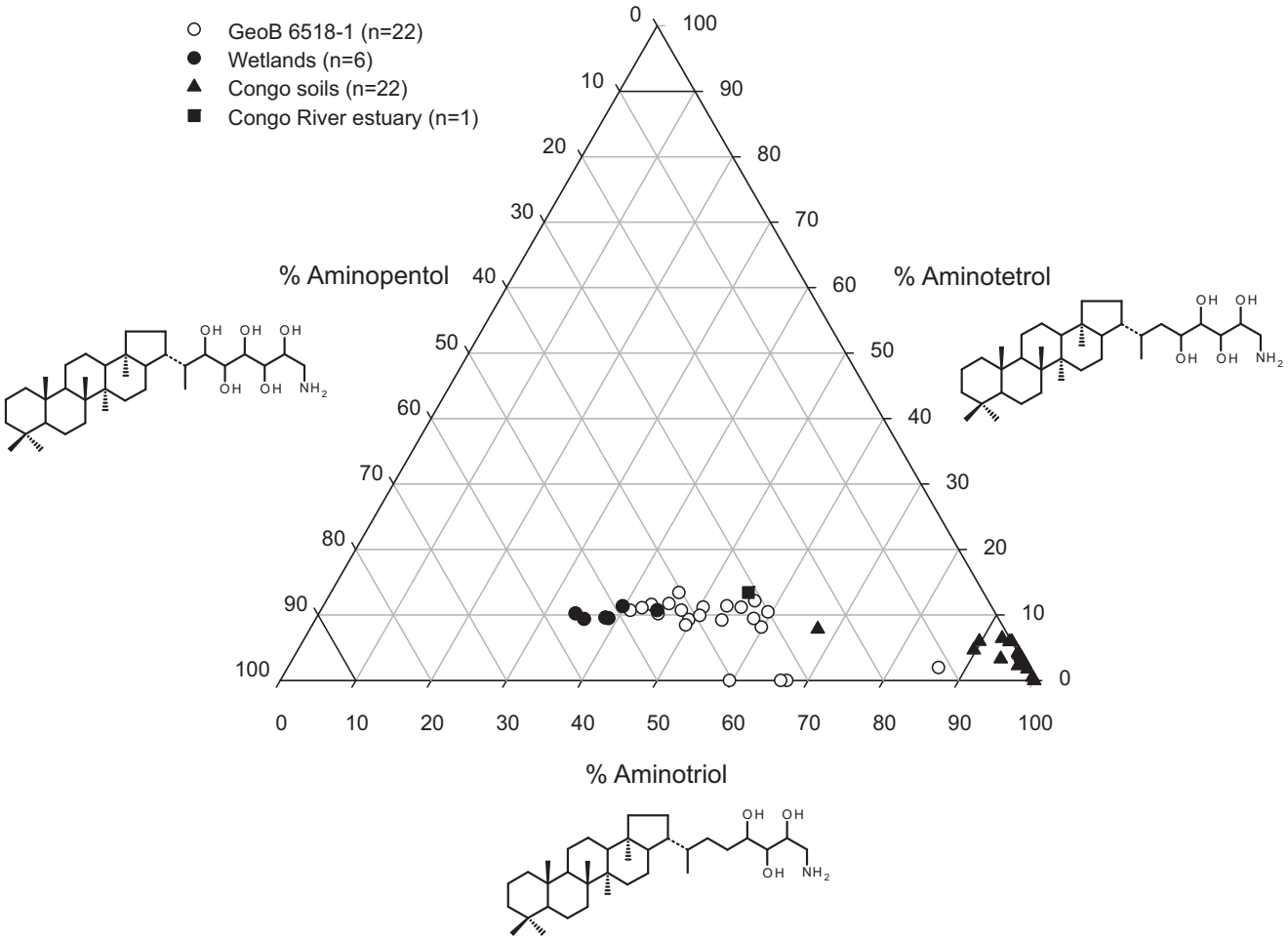

Figure S2: BHP compositions of Congo wetland deposits, soils, and sediments. Ternary plot of the relative abundance of aminoBHP compounds (aminotriol, aminotetrol and aminopentol) present in core GeoB6518-1 (22 samples; this study), the Congo estuarine sediment, 6 wetland sediments and 22 soils from the Congo (data from ref 23).

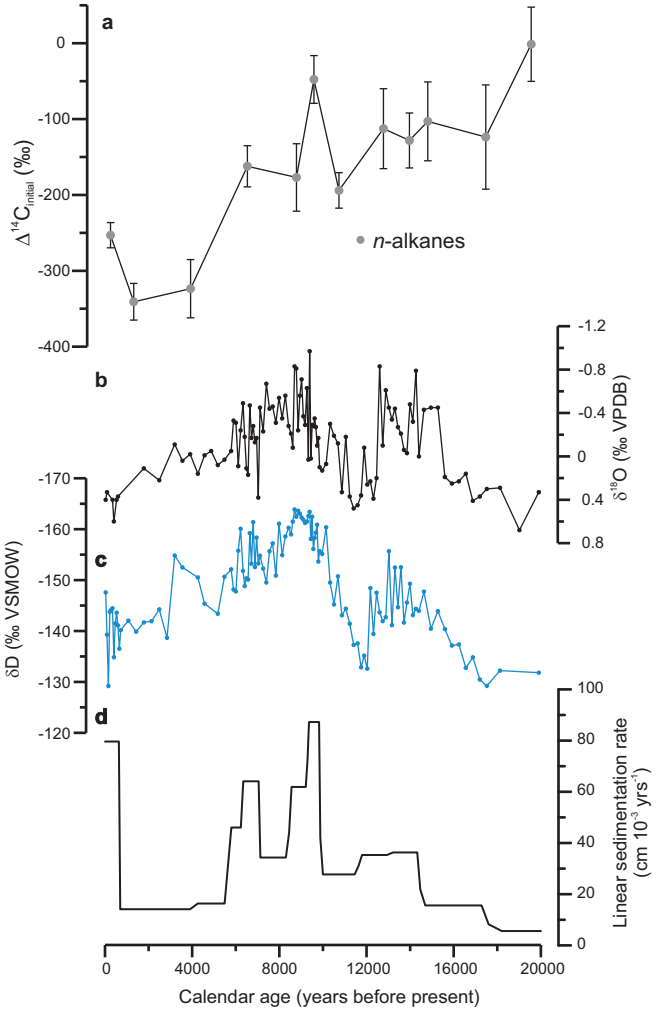

Figure S3: Independence of OM ages, proxy records and sedimentation. Comparison of initial radiocarbon contents of *n*-alkanes in GeoB6518-1 (a) with Congo River runoff reconstructions based on oxygen isotope compositions of planktonic foraminifera (b, black), compound-specific plant-wax based reconstruction of rainfall intensity in the Congo basin[21] (c, blue) and linear sedimentation rate of GeoB6518-1 (d). Error bars in a) reflect analytical uncertainty.